Growth of short fatigue cracks emanating from notches in a two-phase austenitic-ferritic stainless steel

Ondřej Kotecký[1,2,a], Suzanne Degallaix[1,b] and Jaroslav Polák[2,c]

[1] Laboratoire de Mécanique de Lille (UMR CNRS 8107), Bd Paul Langevin, 59651, Villeneuve d'Ascq Cedex, France

[2] Institute of Physics of Materials, Žižkova 22, 61662, Brno, Czech Republic

[a]kotecky@ipm.cz, [b]suzanne.degallaix@ec-lille.fr, [c]polak@ipm.cz

Keywords: notch, fatigue crack shape, growth rate, duplex stainless steel, prediction.

Abstract. The aim of the present work is to study the influence of microstructure and of the stress gradient on the fatigue crack growth in a two-phase austenitic-ferritic stainless steel in specimens with regions of confined plasticity. Direct optical observations and potential drop technique calibrated via the finite element method are used to measure the surface crack size and its depth and to determine the in-depth and surface crack growth. The effect of stress and strain gradients on the crack propagation kinetics and the crack shape is evaluated and discussed.

Introduction

Under fatigue, cracks initiate where stress concentrations exist, then the initiated cracks propagate progressively and lead to fracture of the component. Thus notches represent the most critical regions of a mechanically loaded structure. While for elastically loaded notched structures the fatigue life predictions are more accurate, predictions are particularly difficult when an elastically-plastically loaded region is present. Studies of the short fatigue cracks emanating from stress concentrations [1,2] revealed that, compared to fracture mechanics predictions, small cracks grow at higher rates and bellow the long crack threshold. Depending on the stress level, after initiation such fast growing cracks eventually slow-down or arrest as the crack front leaves the notch plastic zone and the stress and strain diminish. Subsequently, the crack accelerates as the crack-tip plasticity becomes important. Such behaviour is thought of as a two phase process with two superposed driving forces: one controlling the initiation in the notch root and the other the crack growth [2]. The short-crack growth phase in many cases determines the fatigue life [3].

Experimental

Flat specimens of three notch geometries were used to study the kinetics of mechanically short cracks emanating from notches. The surface crack sizes are measured optically and the in-depth dimensions were determined via the direct current potential drop method (dcPD). The dcPD results were calibrated by the finite element method.

   Material. The material studied is a 2507 nitrogen alloyed austenitic-ferritic stainless steel (duplex stainless steel, DSS) supplied by Aubert & Duval in forged bars of 70 mm in diameter. The chemical composition is shown in Table 1. The hot rolling and the solution treatment (1060 °C / 1 h) followed by a water-quenching results in a transverse isotropic two-phase microstructure (see Fig. 3) consisting of elongated islands of austenitic phase (γ, fcc) embedded in the ferritic matrix (α, bcc). Volume fractions are approximately 40 % of the austenitic and 60 % of the ferritic phase. The size of the grains in the austenitic phase lies in the interval from 10 to 20 μm; the grains of the ferritic phase are approximately three times as large. Grains of both phases are slightly elongated in the rolling direction.

Cr	Ni	Mo	N	Mn	Si	C	Cu	Fe
24.7	6.5	2.8	0.17	0.8	0.6	0.02	0.07	bal.

Table 1: Chemical composition (in wt. %) of the duplex stainless steel studied.
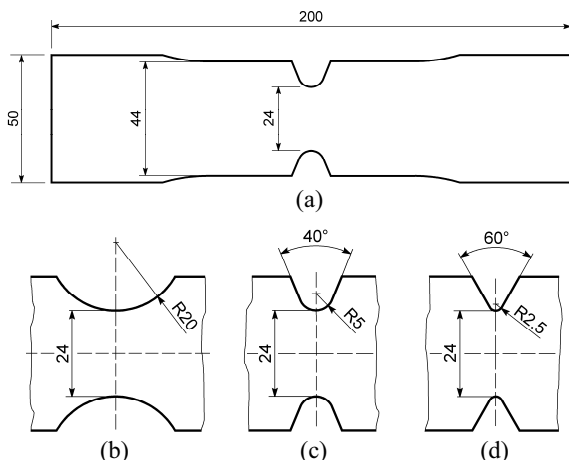
Fig. 1: The specimen geometries. Details of the central part: blunt (b), medium (c) and sharp (d) notches. Not to scale.
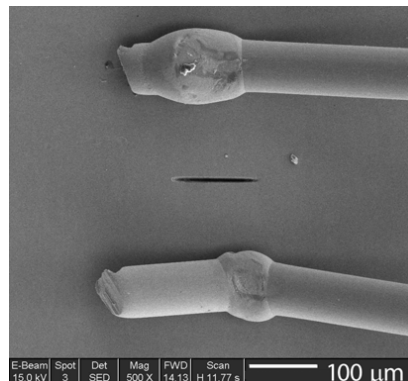
Fig. 2: A SEM image of a FIB-machined pre-crack in the middle of the notch root. The dcPD potential leads are visible.

Specimens. For the study of the kinetics mechanically short cracks double-edged notched flat specimens having 3 mm thickness with three notch geometries were used. For the notch dimensions see Fig. 1. The notch depth and the distance between the notch tips were the same in all three cases. The theoretical stress concentration factors, K_t, were calculated by the finite element method and equal to 1.4, 2.3 and 3.2 for the blunt, medium and sharp notches respectively. The contours were spark-erosion cut. The notch roots were machined, polished and electrochemically etched to reveal the phase boundaries.

Observation methods. To follow the fatigue damage development and crack growth on the surface, observations were made using an optical microscope with a resolution under one micrometer. To study the influence of the stress and strain gradient, in-depth measurements were needed. Because of the stainless nature of the studied material heat tinting could not be used. Attempts to beach-mark using loading blocks with higher loading ratio, R, while maintaining the maximal stress, did not produce any measureable marks on the fracture surface. Moreover, interpretation of crack growth data obtained by this technique would not be straightforward. For these reasons the direct current potential drop (dcPD) technique was adopted. To measure the earliest crack growth possible, the potential induced by a pulsating current of 10 A was measured as close to the crack mouth as possible. High sensitivity to the changes of the crack dimension was gained. The distance between the leads ranged between 220 and 440 μm. In order to localize the fatigue crack initiation a pre-crack had to be machined in between the potential leads. The focused-ion beam (FIB) method machined a semi-elliptical slot approximately 130 μm wide and 35 μm deep (see Fig 2). A second pair of potential leads was used to deal with the dependence of the electrical conductivity on temperature and plasticity. A ratio of the two signals is free of the aforementioned errors. The photographs were taken and the dcPD signal was measured during a short pause in the fatigue test. The measured dcPD signal and the surface crack length were input in

a current-flow finite element model where the geometry of the specimen and the position of the potential leads were carefully reproduced. Iterative calculations yielded the crack depth. A hypothesis of semi-elliptical crack-shape was made. Measurements before and after the crack coalescence were not used for the analysis.

Fatigue testing. Specimens were cyclically loaded with constant nominal stress amplitude, σ_a, and with the load ratio $R = 0.1$. Cycles were sinusoidal with constant frequency $f = 1.5$ Hz. Stress amplitudes were applied so that maximum plastic strain levels after the first quarter-cycle in the notch root, ε_{pNmax}, was the same in the different notch geometries. Three ε_{pNmax} were chosen. The strains were calculated by the finite element method. The maximum local plastic strains, the specimen geometries tested and the experimentally found numbers of cycles to fracture are shown in Table 2. The tests were performed in air at room temperature.

ε_{pNmax}	blunt notch $K_t = 1.4$	medium notch $K_t = 2.3$	sharp notch $K_t = 3.2$
9.0×10^{-3}		2.3×10^{4}	2.9×10^{4}
2.8×10^{-3}	9.4×10^{4}		1.7×10^{5}
5.5×10^{-4}	4.3×10^{5}	4.7×10^{5}	

Table 2: The maximum plastic strain in the notch root for different specimen geometries tested. The three combinations were not tested.

Results and discussion

Relief evolution and surface crack growth. After the first half-cycle only the highly stressed samples with lower K_t (blunt notch at medium strain level and medium notch at high strain level) showed monotonic slip. Then a short crack initiated on both sides of the pre-crack in all specimens before cyclic surface relief formed. The fraction of life to initiation ranged from 1 to 9 percent of the number of cycles to fracture. No clear dependence of the number of cycles to initiation on either the local strain or the strain gradient was observed. The surface angle between the initiated-crack path and the plane of symmetry perpendicular to the loading axis was in most cases between 35 and 55 degrees, see Fig. 3a. In all specimens this crack became the principal crack and led to fracture.

Simultaneously with the growth of the principal crack that initiated from the pre-crack, surface relief evolution was observed in areas far from the crack tip. In the two highly stressed specimens (medium and sharp notch with $\varepsilon_{pNmax} = 9.0 \times 10^{-3}$) the slip witnessed by the persistent slip markings (PSM) appeared during the first thousand cycles. In the specimens stressed by the medium plastic strain level (blunt and sharp notch with $\varepsilon_{pNmax} = 2.8 \times 10^{-3}$) the PSMs appeared after approximately one third of the fatigue life, see Fig. 3b. The specimens strained at the lowest level (medium and blunt notch with $\varepsilon_{pNmax} = 5.5 \times 10^{-4}$) didn't show any optically observable relief except that caused by the crack tip. In general, the PSM appeared first in the austenitic phase and got accentuated during the cycling. In two specimens (medium notch at high strain level and blunt notch at medium strain level), the strain was accommodated by both the austenitic and the ferritic phases. In the highly stressed specimen with the sharp-notch geometry nearly no PSMs were observed in the ferritic phase.
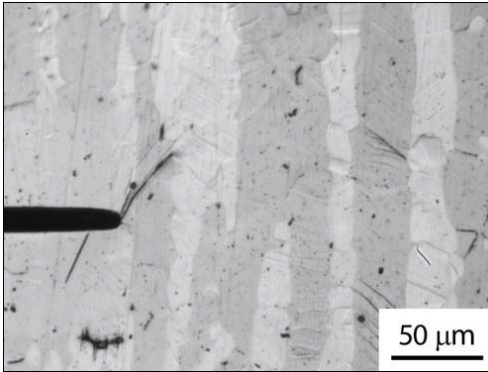
Fig. 3a: Crack initiates from the pre-crack early in fatigue life and grows in a direction close to 45°. Blunt notch, $\varepsilon_{pNmax} = 2.8 \times 10^{-3}$, N = 23 000 ($N = 0.25\ N_f$); loading axis is vertical.
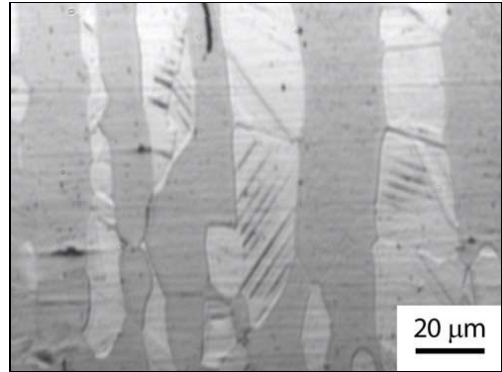
Fig. 3b: Persistent slip markings in the root of a sharp notch. PSMs visible only in the austenitic phase. $\varepsilon_{pNmax} = 2.8 \times 10^{-3}$, $N = 56\ 000$ cycles ($N = 0.33\ N_f$); loading axis is vertical.

Later in the fatigue life, simultaneously with the growth of the principal crack, secondary cracks are initiated. In most cases the initiation takes place in the ferritic phase. In fewer cases the cracks initiate on the austenite-ferrite phase boundary. This observation correspond with the findings of Degallaix *et al.* [4] and El Bartali *et al.* [5], who studied fatigue damage in the DSSs. The number of naturally initiated cracks was approximately the same for samples with steep and shallow stress gradient (sharp and medium notches respectively) for the given plastic strain level. Majority of the cracks became shielded by the principal crack and thus became non-propagating. Only in a few cases such crack coalesced with the principal crack and have substantial impact on the growth rate. This fact is important for the feasibility of the in-depth measurements discussed later.

The above mentioned observations can be explained by the presence of stress and strain gradient under the notch root: due to the sample geometry, the specimens loaded with a stress resulting in the same local plastic strain level on the surface, ε_{pNmax}, the stress gradient is steeper in the specimens with a sharper notch and the notch plastic zone is smaller. As addressed by Neuber [6] and numerically analyzed by Sansoz *et al.* [7], in notched structures loaded with positive load ratio $R > 0$, the mean stress relaxes and the notch root is loaded nearly symmetrically. The volume beyond the notch plastic zone is subjected to different levels of elastic strain.

In-depth crack growth and evolution of the crack shape. The dcPD data together with the surface crack lengths were input in a finite element model which yielded the crack depths and shapes. On the Fig. 4 two representative results of the crack-shape evolution are shown. In the beginning of the fatigue life cracks tend to grow faster in the in-depth direction. From the initial shape of the pre-crack the crack-shape approaches to a semi-circle, in other words the aspect-ratio approaches to one. It appears that there is a value of the aspect ratio – close to 0.8 for the higher amplitudes of local strain and close to 1.0 for the lowest amplitude – at which the in-depth growth slows down. While the aspect ratio of the cracks in the blunt notches still tend to $a/c = 1$, see Fig. 4a, in the sharp notches the aspect ratio decrease, see Fig. 4b. Similar results were observed in tension-compression by Sansoz *et al.* [7] and analyzed in tension and/or bending by Lin and Smith [8]. Sansoz *et al.* studied fatigue crack growth in smooth and notched samples, loaded with $R = 0$, -0.5 and -1. They attribute the crack shape evolution to the crack closure effects. Lin and Smith remarked that the aspect ratio approaches asymptotically a final crack shape that is nearly

ECF17
ECF17

17th European Conference on Fracture
2-5 September, 2008, Brno, Czech Republic

BRNO '08
IX 2 - 5

independent on the shape of the starting defect. This effect is termed the aspect ratio path. They predicted no substantial difference of the aspect ratio path for different notch geometries that we observed.
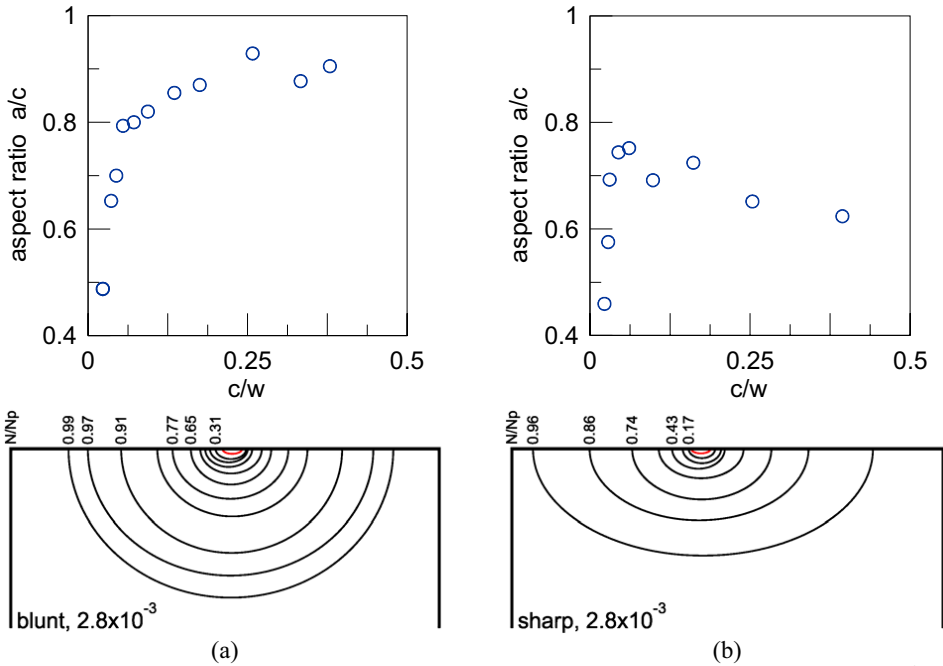
Fig. 4: Evolution of the aspect-ratio a/c in the samples with (a) blunt notch, $\varepsilon_{pNmax} = 2.8 \times 10^{-3}$ and (b) sharp notch, $\varepsilon_{pNmax} = 9.0 \times 10^{-3}$. The horizontal line on the sketch is the notch root and the red contour is the pre-crack.

Kinetics of crack growth. The results are plotted in the Fig. 5. To account for the crack-shape change in the crack growth rates analysis, we use the equivalent crack length (or the radius of an equivalent semi-circular crack), r_{eq}, defined as $r_{eq} = \sqrt{a \cdot c}$, where c is one half of the surface crack length and a is the crack depth. N_p is the number of cycles for the crack to achieve the sample corner.

It appears that when the equivalent crack is plotted against the normalized number of cycles N/N_p, see Fig. 5a, the data points fit in a linear band relying the size of the pre-crack and the final crack length, here one half of the specimen width. The crack growth rates, see Fig. 5b, show three distinct groups of data where in each of them there are two samples tested at the same maximum plastic strain level after the first quarter-cycle in the notch root, ε_{pNmax}. In each group the crack in a specimen with the sharper of the two notch geometries grows slower with increasing crack length. This behavior is due to the stress and strain gradient.
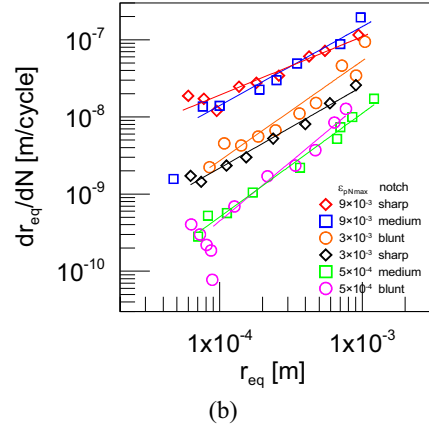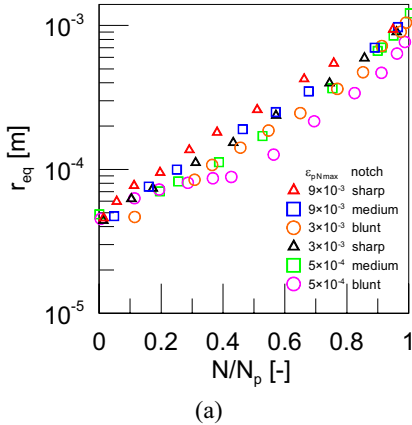
Fig. 5a: Equivalent crack length r_{eq} plotted as a function of N/N_p fit in a linear band.

Fig. 5b: Fatigue crack growth rates can be approximated by a power law with slope close to one.

Polák [9] and Polák and Zezulka [3] conducted fatigue crack growth tests in smooth specimens made from a similar material. Based on the results equivalent to those in Fig. 5a they observed that

$$a = a_i \exp(k_g \, N/N_f), \tag{1}$$

where a_i is the extrapolated value of the crack length to zero cycles. Previous equation can be rewritten as

$$\frac{da}{dN} = k_g \, a_i \exp(k_g \, N/N_f) = k_g \, a. \tag{2}$$

Based on their observations Polák proposed that for smooth specimens the crack growth coefficient, k_g, would be proportional to the plastic strain amplitude

$$k_g = k_{g0} \, \varepsilon_{ap}^{\, d}. \tag{3}$$

Integrating the above equation yields the number of cycles to fracture.

Based on our fatigue tests we observe that

$$\frac{dr_{eq}}{dN} = k_g \, r_{eq}^{\, n} \quad \text{or rewritten} \quad \log\left(\frac{dr_{eq}}{dN}\right) = \log(k_g) + n \, \log(r_{eq}). \tag{4}$$

Since the exponent n is close to one, the above law is close to the Eq. 2.

More fatigue crack growth tests at the same local strain levels would be necessary to get a statistically significant picture of how the stress and strain levels and the gradients influence on the crack growth coefficient, k_g, and the exponent n.

Conclusions

Study of the surface fatigue damage and fatigue crack initiation and short crack growth in notched samples made from an austenitic-ferritic stainless steel permitted us to describe the surface relief

evolution and fatigue crack initiation sites depending on the stress concentration and local strain level.

Use of the direct-current potential-drop method together with a small pre-crack seems to be well suited to study the kinetics of mechanically short cracks emanating from notches and to follow the crack-shape evolution from the early stages of crack propagation. In all specimen geometries a fast in-depth growth in the early stages of crack propagation until a certain aspect-ratio was observed. The following aspect ratio evolution depends on the specimen geometry.

The kinetics of mechanically short cracks emanating from notches are a function of the local strain and show an exponential dependence on the length of the equivalent crack with a slight influence of the stress and strain gradient.

Acknowledgement

References

[1] K. Tanaka, in: *Current research on fatigue cracks*, edited by T. Tanaka, M. Jono and K. Komai: Elsevier Science Pub, New York, NY (1987), 314 p.

[2] R.A. Smith and K.J. Miller: Int. J. Mech. Sci., Vol. 20 (1978), p. 201

[3] J. Polák and P. Zezulka: Fatigue Fract. Engng. Mater. Struct, Vol. 28 (2005), p. 923

[4] S. Degallaix, A. Seddouki, G. Degallaix, T. Kruml and J. Polák: Fatigue Fract. Engng. Mater. Struct., Vol. 18 (1995), p. 65

[5] A. El Bartali, V. Aubin and S. Degallaix: Fatigue Fract. Engng. Mater. Struct., Vol. 31 (2008), p. 137

[6] Neuber, H.: *Kerbspannungslehre*, Springer-Verlag, Berlin (1958)

[7] F. Sansoz, B. Brethes and A. Pineau: Fatigue Fract. Engng. Mater. Struct., Vol. (25) 2002, p. 41

[8] X.B. Lin and R.A. Smith: Eng. Fract. Mech., Vol. 63 (1999), p. 523

[9] J. Polák: Int. J. Fatigue, Vol. 27 (2005), p. 1192